Molecular Crystals and Liquid Crystals

Publication details, including instructions for authors and subscription information:
http://www.tandfonline.com/loi/gmcl16

Perturbation Theroy for Nematic Liquid Crystals of Axially Symmetric Molecules: Properties of a Trial System

S. Singh [a] , Y. Singh [a] , T. Barbara [a] & B. P. Dailey [b]
[a] Department of Physics, Banaras Hindu University, Varanasi, 221005, INDIA
[b] Department of Chemistry, Columbia University, New York, New York, 10027

Version of record first published: 28 Mar 2007.

To cite this article: S. Singh , Y. Singh , T. Barbara & B. P. Dailey (1982): Perturbation Theroy for Nematic Liquid Crystals of Axially Symmetric Molecules: Properties of a Trial System, Molecular Crystals and Liquid Crystals, 87:3-4, 211-237

To link to this article: http://dx.doi.org/10.1080/00268948208084443

Mol. Cryst. Liq. Cryst., 1982, Vol. 87, pp. 211–237
0026-8941/82/8703-0211$06.50/0

Printed in the United States of America

Perturbation Theory for Nematic Liquid Crystals of Axially Symmetric Molecules: Properties of a Trial System

S. SINGH and Y. SINGH

Department of Physics, Banaras Hindu University, Varanasi-221005, INDIA

(Received November 20, 1981)

A statistical mechanical perturbation theory for the equilibrium properties of nematic liquid crystals is presented in which the reference potential function is non-spherical and consists of the short-range rapidly varying repulsive part of the pair potential. Calculations are made for a trial system in which molecules are assumed to interact via a pair potential which has repulsive part represented by a repulsion between hard spherocylinders and an attractive part which is function of only r_{12} and Ω_{12} (r_{12} is the center of mass distance and Ω_{12} the relative orientation between the two molecules), and represent approximately the interaction arising from dispersion interaction between two asymmetric molecules. Assuming that the pair correlation function $g(r_{12}, \Omega_{12})$ for a fluid of hard spherocylinders scales as $g[r_{12}/D(\Omega_{12})]$ where $D(\Omega_{12})$ is angle-dependent range parameter the properties of the reference system and the first order perturbation term are evaluated. The agreement found between the calculated values of the compressibility factor for isotropic phase of fluids of hard spherocylinders and the values obtained from machine simulations is excellent. The functional form and the density dependence of the effective one-body orientational potential $\psi(\Omega)$ is discussed in detail. It is shown that the nematic–isotropic transition properties are very sensitive to the form of $\psi(\Omega)$.

1. INTRODUCTION

Nematic phase usually occurs only with materials which do not distinguish between right and left and the molecules of which have rodlike shape.[1]

Let us consider a system of N axially symmetric nonspherical nematogenic molecules contained in a volume V at temperature T. Let the system be described by a potential function which depends on orientations and relative centers of mass coordinates of molecules but is independent of rotational momenta and internal vibrational states. Since the flexibility of liquid crystal forming molecules (particularly in their alkyl end chains) is believed to be important in many instances, this assumption may not be realistic. It may also be remembered that the symmetry of the nematogenic molecules is never as high as $D_{\infty h}$; real molecules are more lath like than cylindrical.[1] However, for many real systems, the terms in the pair potential energy which result from deviations from cylindrical symmetry are small and can be treated by perturbation.

Assuming that the total potential energy of interaction of the system is pairwise additive, we write

$$U_N(\bar{X}_1, \text{---}, \bar{X}_N) \equiv U_N(\bar{X}^N) = \sum_{1\leq i<j\leq N} U(\bar{X}_i, \bar{X}_j), \tag{1}$$

where the vector $\bar{X}_i = (\bar{r}_i, \Omega_i)$ represents both the position of the center of mass and orientation of the ith molecule. For rodlike molecules the general form of the pair potential $U(\bar{X}_1, \bar{X}_2)$ is a function of five scalar variables;[2,3] r_{12}, $\Omega_1 \cdot \bar{r}_{12}$, $\Omega_2 \cdot \bar{r}_{12}$, $\Omega_1 \cdot \Omega_2$ and $\Omega_1 x \Omega_2 \cdot \bar{r}_{12} \cdot \Omega_1 x \Omega_2 \cdot \bar{r}_{12}$ actually offers only a selection between two signs and is associated strictly with the chiral configuration, and is responsible for the cholesteric phase. $\Omega_1 \cdot \bar{r}_{12}$ and $\Omega_2 \cdot \bar{r}_{12}$ break the symmetry between splay and bend on the microscopic level. In our present development we, however, consider a pair potential which has a repulsive part represented by repulsion between hard spherocylinders and an attractive part which is function of only r_{12} and $\Omega_1 \cdot \Omega_2$. We describe the trial system in Section 3.

A realistic intermolecular pair potential is thought to have a soft repulsive core and a long-range weak attractive tail. An individual molecule feels the combined effects of the long-range tail from many molecules which surround it from all sides. The net effect of the long-range tail in the structure thus tends to cancel out and is very small in comparison to the forces arising from the repulsive cores of the nearest neighboring molecules. This forms the basis of a perturbation expansion developed in Section 2. The theory given here differs in detail from that, recently, developed by one of us.[4] The properties of the reference system are calculated in Section 4. In Section 5 we give expressions for *effective one-body orientational perturbation potential* $\psi(\Omega)$, the Helmholtz free-energy and pressure in the first-order perturbation for the assumed pair potential model. Section 6 defines the conditions for thermodynamic equilibrium. Results and discussions are presented in Section 7.

2. PERTURBATION EXPANSION

In order to apply a perturbation theory to the liquid crystalline phase, we write the pair potential energy of interaction $U(\bar{X}_i, \bar{X}_j)$ as a sum of two parts—one part of this division is known as the reference potential U_0 and the other perturbation potential U_p, i.e.

$$U(\bar{X}_i, \bar{X}_j; \lambda) = U_0(\bar{X}_i, \bar{X}_j) + \lambda\, U_p(\bar{X}_i, \bar{X}_j). \tag{2}$$

$U_0(\bar{X}_i, \bar{X}_j)$ is generally chosen to include the rapidly varying short-range repulsive part of the interaction whereas $U_p(\bar{X}_i, \bar{X}_j)$ contains the more smoothly varying long-range attractive part. λ is a perturbation parameter. For $\lambda = 0$, $U(\bar{X}_i, \bar{X}_j; \lambda)$ reduces to the reference potential, whereas for $\lambda = 1$, $U(\bar{X}_i, \bar{X}_j; \lambda)$ becomes the full potential $U(\bar{X}_i, \bar{X}_j) = U_0(\bar{X}_i, \bar{X}_j) + U_p(\bar{X}_i, \bar{X}_j)$. Thus by increasing the value of λ from 0 to 1, the perturbation is generally switched on.

The configurational integral of the system is

$$Z_N(V, T) = \frac{1}{N!(4\pi)^N} \int d\bar{r}^N \int d\Omega^N \exp[-\beta U_N(\bar{X}_1, \cdots, \bar{X}_N)]. \tag{3}$$

The angular integration of Eq. (3) can be approximated to arbitrary accuracy[5,6] by dividing the unit sphere into arbitrary small sections of solid angle $\Delta\omega (n = 4\pi/\Delta\omega$ is the number of discrete orientations) and summing overall possible orientational distributions $\{N_1, ----, N_p, ----, N_n\}$ where N_p is the number of molecules having orientations falling in the pth solid angle and $\Sigma_{p=1}^{n} N_p = N$. Thus

$$Z_N(V, T) = \frac{1}{N!(4\pi)^N} \sum_{N_1} \cdots \sum_{N_2} \frac{\mathrm{N}!(\Delta\omega)^N}{N_1! \cdots N_n!} \int d\bar{r}^N$$

$$\sum_{p=1}^{n} N_p = N \;\times \exp[-\beta U_N(\bar{r}^N, \tilde{N}_1, \cdots, \tilde{N}_n)]. \tag{4}$$

Here the factor $N!/\Pi_{p=1}^{n} N_p!$ describes the number of ways in which the N molecules can have the distribution of orientations N_1, ---, N_p, ---, N_n. Equation (4) can be approximated to give

$$Z_N(V, T) \simeq \left(\frac{\Delta\omega}{4\pi}\right)^N \left[\prod_{p=1}^{n} \tilde{N}_p\right]^{-1} \int d\bar{r}^N \exp[-\beta U_N(\bar{r}^N, \tilde{N}_1, \cdots, \tilde{N}_n)], \tag{5}$$

where the set $\{\tilde{N}_1, --- ; \tilde{N}_n\}$ corresponds to the maximum term in Eq. (4).

Using Eqs. (2) and (1) we can break the total potential energy of interaction into two parts, i.e.

$$U_N(\bar{r}^N; \tilde{N}_1, \cdots, \tilde{N}_n) = U_N^{(0)}(\bar{r}^N; \tilde{N}_1, \cdots, \tilde{N}_n) + \lambda U_N^{(p)}(\bar{r}^N, \tilde{N}_1, \cdots, \tilde{N}_n). \quad (6)$$

Thus

$$Z_N(V, T) = \left(\frac{\Delta\omega}{4\pi}\right)^N \left[\prod_{p=1}^{n} \tilde{N}_p!\right]^{-1} \int d\bar{r}^N \exp[-\beta U_N^{(0)}(\bar{r}^N; \tilde{N}_1, \cdots, \tilde{N}_n)] \times \exp[-\beta\lambda U_N^{(p)}(\bar{r}^N; \tilde{N}_1, \cdots, \tilde{N}_n)], \quad (7)$$

and

$$\frac{\partial \ln Z_N}{\partial \lambda} = -\frac{1}{2V}\beta \sum_{p=1}^{n} \sum_{p'=1}^{n} \tilde{N}_p \tilde{N}_{p'} \int d\bar{r}\, U_p(\bar{r}, \Omega_p, \Omega_{p'}) g(\bar{r}, \Omega_p, \Omega_{p'}), \quad (8)$$

where

$$g(\bar{r}, \Omega_p, \Omega_{p'}) = \frac{V^2}{Z_N(V, T)} \left(\frac{\Delta\omega}{4\pi}\right)^N \left[\prod_{p=1}^{n} \tilde{N}_p!\right]^{-1} \times \int \exp[-\beta U_N(\bar{r}^N; \tilde{N}_1, \cdots, \tilde{N}_n; \lambda)] \, d\bar{r} \tilde{N}_1 \cdots d\bar{r} \tilde{N}_{p-1} d\bar{r} \tilde{N}_{p'-1} \cdots d\bar{r} \tilde{N}_n. \quad (9)$$

Integration of Eq. (8) leads to

$$\ln Z_N(V, T) = \ln Z_N^0(V, T) - \frac{1}{2V}\beta \int_0^1 d\lambda \sum_{p=1}^{n} \tilde{N}_p \sum_{p'=1}^{n} \tilde{N}_{p'} \times \int d\bar{r}\, U_p(\bar{r}, \Omega_p, \Omega_{p'}) g(\bar{r}, \Omega_p, \Omega_{p'}; \lambda). \quad (10)$$

We choose a continuous function $f(\Omega)$ to describe the orientational distribution such that

$$\tilde{N}_p = N f(\Omega_p) d\Omega_p. \quad (11)$$

Using the relationship $A = -\mathrm{kT} \ln Z_N(V, T)$ for the Helmholtz free-energy, we get[7,8]

$$\frac{\beta A}{N} = \frac{\beta A^{(0)}}{N} + \frac{1}{2}\beta\rho \int_0^1 d\lambda \int f(\Omega_p) d\Omega_p \int f(\Omega_{p'}) d\Omega_{p'} \int d\bar{r}\, U_p(\bar{r}, \Omega_p, \Omega_{p'}) g(\bar{r}, \Omega_p, \Omega_{p'}; \lambda). \quad (12)$$

If we define effective one-body orientational perturbation potential $\psi(\Omega)$ by the relation

$$\psi(\Omega_p) = \frac{1}{2}\rho \int_0^1 d\lambda \int d\Omega_{p'} f(\Omega_{p'}) \int d\bar{r}\, U_p(\bar{r}, \Omega_p, \Omega_{p'}) g(\bar{r}, \Omega_p, \Omega_{p'}, \lambda), \tag{13}$$

Eq. (12) can be rewritten as

$$\frac{\beta A}{N} = \frac{\beta A^{(0)}}{N} + \beta \int d\Omega_p f(\Omega_p) \psi(\Omega_p). \tag{14}$$

By expanding $g(\bar{r}, \Omega_p, \Omega_{p'}; \lambda)$ and A in powers of λ;

$$g(\bar{r}, \Omega_p, \Omega_{p'}; \lambda) = g^{(0)}(\bar{r}, \Omega_p, \Omega_{p'}) + \lambda g^{(1)}(\bar{r}, \Omega_p, \Omega_{p'}) + \cdots, \tag{15}$$

$$A = A^{(0)} + \lambda A^{(1)} + \lambda^2 A^{(2)} + \cdots, \tag{16}$$

and inserting these expressions into (12) one gets on equating the coefficients of λ's from both sides

$$\frac{\beta A^{(s)}}{N} = \frac{1}{2s} \beta\rho \int f(\Omega_p) d\Omega_p \int f(\Omega_{p'}) d\Omega_{p'} \int d\bar{r} \times U_p(\bar{r}, \Omega_p, \Omega_{p'}) g^{(s-1)}(\bar{r}, \Omega_p, \Omega_{p'}), \tag{17}$$

where s denotes the order of perturbation. All *zero*th order terms refer to quantities corresponding to the reference system. The perturbation series for the Helmhotz free-energy can now be rewritten as

$$\frac{\beta A}{N} = \frac{\beta A^{(0)}}{N} + \sum_{s=1}^{\infty} \frac{\beta A^{(s)}}{N}. \tag{18}$$

In the first order of perturbation,

$$\psi^{(1)}(\Omega_p) = \frac{1}{2}\rho \int d\Omega_{p'} f(\Omega_{p'}) \int d\bar{r}\, U_p(\bar{r}, \Omega_p, \Omega_{p'}) g^{(0)}(\bar{r}, \Omega_p, \Omega_{p'}), \tag{19}$$

where $g^{(0)}(\bar{r}, \Omega_p, \Omega_{p'})$ is the pair correlation function (PCF) for the reference system. For an isotropic reference potential $U_0(r)$, $g^0(\bar{r}, \Omega_p, \Omega_{p'})$ will be independent of Euler angles Ω_p and $\Omega_{p'}$, i.e.

$$g^{(0)}(\bar{r}, \Omega_p, \Omega_{p'}) = g^{(0)}(r). \tag{20}$$

Therefore

$$\psi^{(1)}(\Omega_p) = \frac{1}{2}\rho \int d\Omega_{p'} f(\Omega_{p'}) \int d\bar{r}\, U_p(\bar{r}, \Omega_p, \Omega_{p'}) g^{(0)}(r), \tag{21}$$

and correct to the first-order of perturbation,

$$\beta A \simeq \beta A^{(0)} + N\beta \int f(\Omega_p) d\Omega_p \psi^{(1)}(\Omega_p). \tag{22}$$

We thus see that if the reference pair potential U_0 is taken to represent the isotropic part of the pair potential and the perturbation potential U_p the anisotropic part, the first-order perturbation theory reduces to molecular field theory as formulated by Woo and coworkers[3] and Luckhurst.[9]

In what they call *generalized Van der Waals* theory Gelbert and Baron[10] and Cotter[5] have assumed $g^{(0)}(\bar{r}, \Omega_p, \Omega_{p'}) \simeq \exp[-\beta U_0(\bar{r}, \Omega_p, \Omega_{p'})]$ and have calculated the effective one-body orientational potential by averaging over the pair attraction which excludes all relative positions denied to pair of molecules because of their anisotropic hard cores. This leads to an effective one-body orientational attractive potential in which the dominant contribution to the angle dependent part comes from the isotropic dispersion attraction contrary to the molecular field version of $\psi^{(1)}(\Omega)$ in which the angle dependent contribution comes solely from anisotropic part of pair interactions. However, the assumption $g^{(0)}(\bar{r}, \Omega_p, \Omega_{p'}) \simeq \exp[-\beta U_0(\bar{r}, \Omega_p, \Omega_{p'})]$ does not hold good at liquid densities.

The observation of Cotter[6] that $\psi(\Omega)$ must be proportional to the first power of number density ρ in order to satisfy the statistical self-consistency has been shown to be incorrect by Singh.[4] It has been shown explicitly that the statistical self-consistency is always satisfied in perturbation expansion as long as the total pair correlation function is taken into account in the calculation of $\psi(\Omega)$.

3. PAIR POTENTIAL MODEL AND THE TRIAL SYSTEM

The method which we describe in this paper is applicable to the classical fluids for which $U_0(\bar{r}_{12}, \Omega_1, \Omega_2)$ contains a harshly repulsive part of the interaction. In saying that the potential U_0 is "short ranged and harshly repulsive" we mean that the Boltzman factor for U_0, $\exp[-\beta U_0(\bar{r}_{12}, \Omega_1, \Omega_2)]$, closely resembles the Boltzmann factor for a hard-core interaction [which is a step function arising from 0 to 1 at a distance corresponding to a distance of closest approach $D(\Omega_1, \Omega_2)$ of two molecules with orientations Ω_1 and Ω_2].

There are two major reasons for separating the pair potential into a harshly repulsive reference potential plus a slowly varying perturbation. First, a fluid of *long-elongated molecules* in which the interactions are short-ranged and harshly repulsive is obviously similar to a fluid of hard rods (hard spheres in the case of simple liquids). It is thus possible to exploit this similarity and define a new fluid, called trial system, in which the pair interaction is given by

$$U_T(\bar{r}_{12}, \Omega_1, \Omega_2) = U_{\mathrm{hr}}(\bar{r}_{12}, \Omega_1, \Omega_2) + U_p(\bar{r}_{12}, \Omega_1, \Omega_2), \qquad (23)$$

where $U_{\mathrm{hr}}(\bar{r}_{12}, \Omega_1, \Omega_2)$ represents the repulsion between hard-spherocylinders of length 2b and diameter 2a (the length to width ratio $x = 2b/2a$). Thus $U_{\mathrm{hr}}(\bar{r}_{12}, \Omega_1, \Omega_2) = \infty$ for any r_{12}, Ω_1, and Ω_2 such that the rods 1 and 2 overlap and equal to zero otherwise. The perturbation potential U_p has the following form:

$$U_p(\bar{r}_{12}, \Omega_1, \Omega_2) = -\frac{1}{r_{12}^6}[C_i + C_a P_2(\cos\theta_{12})],$$

$$\text{for} \quad r_{12} > D(\Omega_1, \Omega_2), \qquad (24)$$

where C_i and C_a are constants related with the isotropic and anisotropic dispersion interactions and θ_{12} is the angle between the orientations of the two molecules.

We call this the trial system because it is necessary to try to find the value of the distance of closest approach $D(\Omega_1, \Omega_2)$. For distances smaller than $D(\Omega_1, \Omega_2)$ the perturbation in the trial system U_T, can take on any finite value. The trial system differs from the fluid of interest only in that the U_0 has been replaced by hard-rod potential U_{hr}. This difference makes the trial system more amenable to the statistical mechanical analysis than the actual liquid of interest.

The second reason for separating $U(\bar{r}_{12}, \Omega_1, \Omega_2)$ into a harshly repulsive reference potential plus a slowly varying perturbation has to do with the convergence of the perturbation series. The convergence of the series depends on the choice of the reference system. A useful theory is one which converges at the first-order term. For simple liquids (a liquid the molecule of which interact via a spherically symmetric pair potential) such convergence has been obtained by selecting the reference potential to represent that part of the pair potential which gives rise to repulsive force and vanishes when this force vanishes.[11] For nematic liquids, it is believed that a suitable choice for the reference potential which will give the required convergence would be the one which includes all the anisotropy of the repulsive core. The effect of the slowly varying attractive potential on the structure of the liquid is small and can be approximated by the first-order perturbation.[12]

4. PROPERTIES OF THE REFERENCE SYSTEM

There have been numerous attempts, in last few years, to calculate the thermodynamic properties of fluids of hard-spherocylinders but most of them introduce unrealistic approximations such as virial expansion,[13] limiting the particles to finite orientations or positions.[14] Methods based on rigorous models such as reference interaction site model[15] (RISM) are computationally too involved to be feasible. The scaled particle theory[5] (SPT) which has widely been used to study the properties of nematic–isotropic transition[10,16] was found to over-estimate significantly the pressure for an isotropic fluid (see Table I) of hard rods as the liquid densities are approached.

In order to estimate the thermodynamic properties of hard spherocylinders we begin with the pressure equation

$$\frac{\beta p_0}{\rho} = 1 - \frac{1}{6}\beta\rho\int d\bar{r}\int f(\Omega_1)d\Omega_1\int f(\Omega_2)d\Omega_2 \times [r\nabla U_0(\mathbf{r}_{12}, \Omega_{12})]g^{(0)}(r_{12}, \Omega_{12}), \quad (25)$$

in which the operator ∇ acts only on the $\mathbf{r}_{12}$ coordinates of $U_0(\mathbf{r}_{12}, \Omega_{12})$. The hard-spherocylinder potential $U_0(\mathbf{r}_{12}, \Omega_{12})$ satisfies the relation:

$$\begin{aligned} U_0(\mathbf{r}_{12}, \Omega_{12}) &= U_0[r_{12}/D(\Omega_{12})] \\ &= U_0(r_{12}^*) = \begin{cases} \infty \text{ for } r^* < 1 \\ 0 \text{ for } r^* > 1 \end{cases}, \end{aligned} \quad (26)$$

where $D(\Omega_{12})$ is the distance of closest approach of two molecules with

TABLE I

Compressibility factor for an isotropic liquid composed of spherocylindrical molecules.

		$\beta p/\rho$		
x	η	a	b	c
2.0	0.3	4.48	4.64	4.48
	0.4	8.20	8.51	7.93
	0.5	15.20	16.88	15.04
	0.6	—	37.60	31.72
3.0	0.3	5.40	5.51	5.24
	0.4	9.60	10.42	9.69
	0.5	18.00	21.12	18.61
	0.6	—	47.85	38.53

a. = Monte-Carlo simulation[18] values.
b. = Values obtained using the scaled particle theory[5] (SPT).
c. = Values obtained using the Eq. (32).

relative orientation Ω_{12}. The Boltzmann factor for U_0, $\exp[-\beta U_0(\mathbf{r}_{12}, \Omega_{12})]$, is a step function arising from 0 to 1 at the distance $D(\Omega_{12})$. Thus

$$-\beta \nabla U_0(\mathbf{r}_{12}, \Omega_{12}) = \delta(r_{12}^* - 1). \tag{27}$$

Following Parson[17] we assume that

$$g^{(0)}(r_{12}, \Omega_{12}) = g^{(0)}[r_{12}/D(\Omega_{12})] = g^{(0)}(r_{12}^*). \tag{28}$$

Though this approximation introduces anisotropy in the pair correlation and is exact at very low density, since $g(r_{12}^*) \sim \exp[-\beta U_0(r_{12}, \Omega_{12})]$, cannot be exact at liquid density. In fact g of the nematic phase must depend on $f(\Omega)$ as well as on r/D. The error in using Eq. (28) at high density is difficult to assess but as shown below it yields compressibility factor for isotropic phase which are in very good agreement with the values obtained from machine simulation[18] (see Table I). It, therefore, appears to us that Eq. (28) can be used to calculate the thermodynamic properties of fluids of elongated molecules even though it does not represent exactly the pair correlation functions. Substitution of Eqs. (27) and (28) in Eq. (25) leads to

$$\frac{\beta p_0}{\rho} = 1 + \frac{1}{2}\rho g_{Hs}(1)\int f(\Omega_1)d\Omega_1 \int f(\Omega_2)d\Omega_2\, V_{exc}, \tag{29}$$

where

$$\begin{aligned} V_{exc} &= \frac{1}{3}\int D^3(\Omega_{12})d\hat{r}_{12} \\ &= 8\, v_0(1-\chi^2)^{-1/2}(1-\chi^2\cos^2\theta_{12})^{1/2}. \end{aligned} \tag{30}$$

$g_{Hs}(1)$ is the value of the radial distribution function of hard sphere at core, v_0 the volume of a molecule and

$$\chi = \frac{x^2-1}{x^2+1}, \tag{31}$$

where x is length to width ratio of a hard-spherocylinder. From Eq. (29), one gets

$$\frac{\beta p_0}{\rho} = 1 + \frac{2\eta(2-\eta)}{(1-\eta)^3}[F_1(\chi) - F_2(\chi)S^2], \tag{32}$$

where

$$\eta = \rho v_0,\ F_1(\chi) = (1-\chi^2)^{-1/2}\left[1 - \frac{1}{6}\chi^2 - \frac{1}{40}\chi^4 - \frac{1}{112}\chi^6 - \cdots\right], \tag{33}$$

and

$$F_2(\chi) = \frac{1}{3}\chi^2(1-\chi^2)^{-1/2}\left[1 + \frac{3}{14}\chi^2 + \frac{5}{64}\chi^4 + \cdots\right]. \quad (34)$$

The value of pressure found from Eq. (32) for isotropic phase is given in column 5 of Table I. We see that these values agree satisfactorily with the quasi-experimental data.[18] Unfortunately, no such data exists for nematic phase and therefore comparison is not possible.

The Helmholtz free-energy per particle for the reference system is given by

$$\frac{\beta A_0}{N} = [\ln \rho - 1] + \int f(\Omega) \ln [4\pi f(\Omega)] d\Omega + H(\rho, U_0), \quad (35)$$

where the first two-terms represent the free-energy of a gas of non-interacting rods and H is the excess free-energy arising from the inter-particle interaction. Thus,

$$H(\rho, U_0) = \int_0^\rho \left(\frac{\beta P_0}{\rho} - 1\right)\frac{d\rho}{\rho}. \quad (36)$$

Here Eq. (36) is solved with the help of Eq. (32). Finally, one gets from Eq. (35),

$$\frac{\beta A_0}{N} = (\ln \rho - 1) + \langle \ln [4\pi f(\Omega)] \rangle + \frac{\eta(4-3\eta)}{(1-\eta)^2}[F_1(\chi) - F_2(\chi)S^2]. \quad (37)$$

Other thermodynamic properties can be calculated by using Eqs. (32) and (37) and the standard thermodynamic relations.

5. FIRST-ORDER PERTURBATION TERM

The Helmholtz free-energy in the first-order perturbation is

$$\frac{\beta A^{(1)}}{N} = \beta \int d\Omega f(\Omega)\, \psi^{(1)}_{(\Omega)}, \quad (38)$$

where $\psi^{(1)}(\Omega)$ is given by Eq. (19) and $U_p(\bar{r}_{12}, \Omega_{12})$ by Eq. (24). Let

$$Y(\Omega_{12}) = -\int d^3r \frac{1}{r^6}[C_i + C_a P_2(\cos\theta_{12})] g^{(0)}(r_{12}, \Omega_{12}). \quad (39)$$

Reducing the distance variables with $D(\Omega_{12})$, we get

$$Y(\Omega_{12}) = -\int_0^\infty dr^* r^{*-4}[C_i + C_a P_2(\cos\theta_{12})] \times g^{(0)}(r^*_{12}) \int \frac{d\hat{r}}{D^3(\Omega_{12})}. \tag{40}$$

Taking the Berne and Peckukas[19] expression for $D(\hat{r}, \Omega_{12})$,

$$D(\hat{r}, \Omega_{12}) = D_0 \times \left[1 - \chi \frac{(\hat{r}\cdot\hat{e}_1)^2 + (\hat{r}\cdot\hat{e}_2)^2 - 2\chi(\hat{r}_1\cdot\hat{e}_1)(\hat{r}_2\cdot\hat{e}_2)(\hat{e}_1\cdot\hat{e}_2)}{1 - \chi^2(\hat{e}_1\cdot\hat{e}_2)^2}\right]^{-1/2}, \tag{41}$$

where $\hat{e}_1$ and $\hat{e}_2$ are unit vectors along the symmetry axes of two interacting spheroids and $D_0 = 2a$. We have evaluated the second integral of Eq. (40) for fixed relative orientation $\hat{e}_1\cdot\hat{e}_2 = \cos\theta_{12}$ and present our results in the following form

$$D_0^3 \int \frac{d\hat{r}}{D^3(\hat{r}, \Omega_{12})} = A_0 + A_2 P_2(\cos\theta_{12}) + A_4 P_4(\cos\theta_{12}) + A_6 P_6(\cos\theta_{12}) + \cdots. \tag{42}$$

The values of constants A_n as a function of length to width ratio x are given in Table II.

TABLE II

The values of the constants of Eq. (42) as a function of length and width ratio x.

x	A_0	A_2	A_4	A_6	A_8	A_{10}	A_{12}
1.5	8.516645	0.815366	0.054715	0.003059	0.000157	0.000007	—
2.0	6.670528	1.458471	0.269592	0.041674	0.005919	0.000815	0.000112
2.5	5.662300	1.698331	0.515333	0.131123	0.030665	0.007200	0.001659
3.0	5.046091	1.728043	0.709363	0.244636	0.077588	0.025913	0.008150
3.5	4.639188	1.663512	0.838436	0.355472	0.138811	0.060275	0.023245
4.0	4.354898	1.561254	0.913193	0.449784	0.205141	0.109477	0.048619
4.5	4.147552	1.447809	0.948115	0.523478	0.269523	0.170383	0.083750
5.0	3.991126	1.335391	0.955612	0.577525	0.328434	0.239177	0.126743
5.5	3.869864	1.229376	0.945038	0.614915	0.380470	0.312293	0.175201
6.0	3.773742	1.131853	0.923083	0.639072	0.425513	0.386804	0.226803
6.5	3.696128	1.043325	0.894405	0.653151	0.464076	0.460502	0.279580
7.0	3.632478	0.963549	0.862183	0.659791	0.496921	0.531831	0.332004
7.5	3.579588	0.891942	0.828555	0.661090	0.524856	0.599776	0.382974
8.0	3.535142	0.827793	0.794922	0.65857	0.548640	0.663740	0.431746
8.5	3.497425	0.770363	0.762179	0.653703	0.568940	0.723432	0.477866
9.0	3.465143	0.718941	0.730871	0.647117	0.586327	0.778781	0.521096
9.5	3.437306	0.672864	0.701303	0.639549	0.601280	0.829866	0.561353
10.0	3.413139	0.631533	0.673617	0.631562	0.614197	0.876858	0.598660

From Eqs. (40) and (42), we get

$$Y = -\frac{1}{D_0^3}[C_i + C_a P_2(\cos\theta_{12})][A_0 + A_2 P_2(\cos\theta_{12}) + A_4 P_4(\cos\theta_{12}) + \cdots]I_6(\rho, T), \quad (43)$$

where

$$I_6(\rho, T) = \int_0^\infty r^{*-4} g_{Hs}^{(0)}(r^*)\,dr^*. \quad (44)$$

The value of I_6 can be obtained from the integral (44) by using the exact radial distribution function for hard spheres obtained from computer simulations. Combining the known density expansion for $g_{Hs}^{(0)}(r^*)$ with the Monte-Carlo values Larsen *et al.*[20] have found the following extended series

$$I_6(\rho^*) = \frac{1}{4\pi}[4.1838 + 2.8287\rho^* + 0.8331\rho^{*2} + 0.0317\rho^{*3} + 0.0858\rho^{*4} - 0.0846\rho^{*5}], \quad (45)$$

where

$$\rho^* = \frac{6}{\pi}\rho v_0.$$

Substituting Eqs. (40), (42) and (44) into Eq. (21) and after some mathematical manipulations, we get

$$\psi^{(1)}(\cos\theta_1) = -\phi_0 - \phi_2 S_2 P_2(\cos\theta_1) - \phi_4 S_4 P_4(\cos\theta_1) + \cdots, \quad (46)$$

where

$$\phi_0 = \frac{1}{12}\pi\eta I_6(\eta)\chi C_i^*\left(A_0 + \frac{1}{5}\frac{C_a^*}{C_i^*}A_2\right), \quad (47a)$$

$$\phi_2 = \frac{1}{12}\pi\eta I_6(\eta)\chi C_i^*\left[A_2 + \left(A_0 + \frac{2}{7}A_2 + \frac{2}{7}A_4\right)\frac{C_a^*}{C_i^*}\right], \quad (47b)$$

$$\phi_4 = \frac{1}{12}\pi\eta I_6(\eta)\chi C_i^*\left[A_4 + \left(\frac{18}{35}A_2 + \frac{20}{27}A_4\right)\frac{C_a^*}{C_i^*}\right], \quad (47c)$$

$$S_n = \int f(\Omega_2)\,d\Omega_2 P_n(\cos\theta_2), \quad (48)$$

and

$$C_i^* = C_i/v_0^2, \quad C_a^* = C_a/v_0^2.$$

In Table III we give the values of ϕ_0, ϕ_2 and ϕ_4 for $x = 1, 2$ and 3 at four packing fraction values 0.3, 0.4, 0.5 and 0.6. We see that the average contribution of ϕ_4 increases with x, it is about 17% with respect to ϕ_2 for $x = 2$ and about 38% for $x = 3$. We thus see that even though the anisotropy in pair interaction is truncated at the second-rank term of the spherical harmonics, the effective one-body orientational perturbation potential has higher-order terms. For $x \geqslant 2$, the contributions of these higher order terms are substantial and cannot be neglected.

In Figures 1 and 2 we plot for several values of x and for $C_l^*/C_a^* = 8$, $\log(2\phi_2^*)$ and $\log(2\phi_4^*)$ as a function of $\log v^*$ where $\phi_n^* = \phi_n/C_l^*$ and $v^* = 1/\rho^*$. These plots are reasonably linear, especially, in view of the large variation in the volume. Consequently, we may write the volume dependence of ϕ_2^* and ϕ_4^* as

$$\phi_2^* = K_1 v^{-\gamma_1}, \tag{49a}$$

and

$$\phi_4^* = K_2 v^{-\gamma_2}. \tag{49b}$$

The slopes of the lines in Figures 1 and 2 yield values for $\gamma_1 = \gamma_2 \simeq 1.63$. We find that while the values of γ_1 and γ_2 are independent of x, K_1 and K_2 depend strongly on x. The dependence of K_n on x is mainly due to the coupling of the hard rods with the isotropic attraction.

In this paper we assume that $\psi(\Omega)$ can be approximated by the first two terms of Eq. (46), i.e.,

$$\psi(\Omega) \simeq -\phi_0 - \phi_2 S_2 P_2(\cos\theta_1). \tag{50}$$

TABLE III

The values of function ϕ_0^*, ϕ_2^*, ϕ_4^* and ϕ_4/ϕ_2 (as defined in Eq. (47) as a function of packing fraction η and length-to-width ratio x for $C_l^*/C_a^* = 8$. $\phi_n^* = \phi_n/C_l^*$

x	η	ϕ_0^*	ϕ_2^*	ϕ_4^*	ϕ_4/ϕ_2
1.0	0.3	0.478543	0.059817	0	0
	0.4	0.718096	0.089762	0	0
	0.5	1.005503	0.125687	0	0
	0.6	1.343454	0.167931	0	0
2.0	0.3	0.510821	0.182006	0.029574	0.1624
	0.4	0.766532	0.273117	0.044379	0.1624
	0.5	1.073397	0.382428	0.062142	0.1624
	0.6	1.434071	0.510963	0.083028	0.1624
3.0	0.3	0.581419	0.279423	0.101235	0.3623
	0.4	0.872471	0.419299	0.151912	0.3623
	0.5	1.222953	0.587117	0.212712	0.3623
	0.6	1.632268	0.784449	0.284206	0.3623

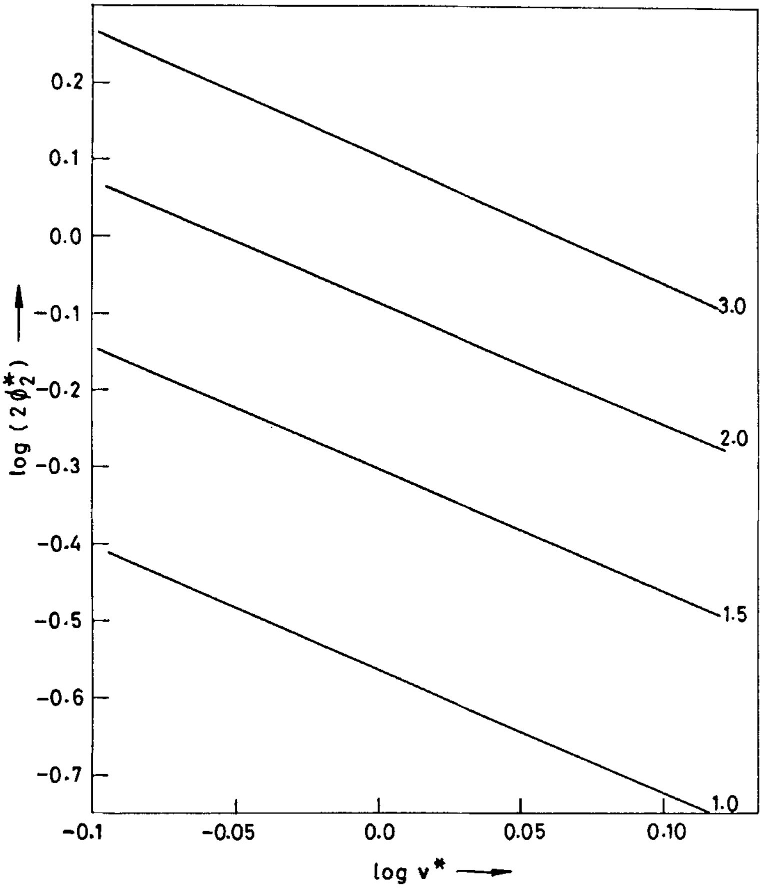

FIGURE 1 The volume dependence of the interaction parameter ϕ_2^* for effective one-body orientational parameter for $C_i^*/C_a^* = 8$. The number on the curves indicates the values of x.

Therefore the calculation presented here are valid for $x \leqslant 2$ only. Under this approximation, the free-energy is given as

$$\frac{\beta A^{(1)}}{N} = -\beta\phi_0 - \beta\phi_2 S_2^2. \tag{51}$$

The first order perturbation correction to the compressibility factor is found to be

$$\frac{\beta p^{(1)}}{\rho} = \beta t_0 + \beta t_2 S_2^2, \tag{52}$$

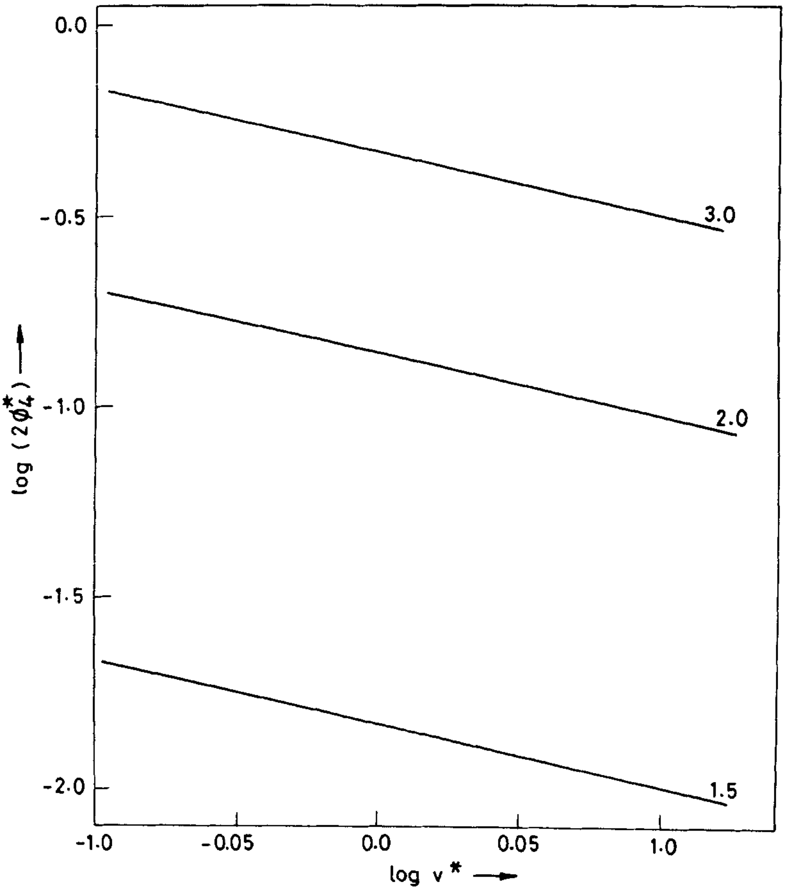

FIGURE 2 The volume dpendence of the interaction parameter ϕ_4^* for effective one-body orientational parameter for $C_i^*/C_a^* = 8$. The number on the curves indicates the values of x.

where

$$t_0 = L\left(A_0 + \frac{1}{5}\frac{C_a^*}{C_i^*}A_2\right), \tag{53a}$$

$$t_2 = L\left[A_2 + \left(A_0 + \frac{2}{7}A_2 + \frac{2}{7}A_4\right)\frac{C_a^*}{C_i^*}\right], \tag{53b}$$

with

$$L = -\frac{1}{12}\pi\eta\chi C_i^*\left[I_6(\eta) + \eta\frac{\partial I_6(\eta)}{\partial\eta}\right]. \tag{53c}$$

Here and onward the subscript 2 has been dropped from S_2. Expressions for the chemical potential and other thermodynamic properties can be derived using the standard thermodynamic relations.

6. THERMODYNAMIC EQUILIBRIUM

Employing the relations (37) and (51) we get the following relations for the total configurational Helmholtz free-energy

$$\frac{\beta A}{N} = \langle \ln [4\pi f(\Omega)] \rangle + C_2 - B_2 S^2, \tag{54}$$

where

$$C_2 = \ln \rho - 1 + \frac{\eta(4-3\eta)}{(1-\eta)^2} F_1(\chi) - \beta\phi_0, \tag{55}$$

and

$$B_2 = \frac{\eta(4-3\eta)}{(1-\eta)^2} F_2(\chi) + \beta\phi_2. \tag{56}$$

The one-particle orientational distribution at a given temperature and pressure is determined by minimizing the free-energy with respect to the variations of $f(\Omega)$ subject to constraint:

$$\int f(\Omega)\, d\omega = 1. \tag{57}$$

From Eqs. (54) and (57) the form of $f(\Omega)$ is readily derived,

$$f(\Omega) = \frac{\exp[2B_2 S P_2(\cos\theta)]}{\int \exp[2B_2 S P_2(\cos\theta)]\, d\Omega}. \tag{58}$$

For the order-parameter of lowest order we now have

$$S = \frac{\int P_2(\cos\theta) \exp[2B_2 S P_2(\cos\theta)]\, d\Omega}{\int \exp[2B_2 S P_2(\cos\theta)]\, d\Omega}. \tag{59}$$

The above equation represents a transcendental equation for the lowest-order parameter $S = \langle P_2(\cos\theta) \rangle$. It is found that when $2B_2 > 4.54$ there are two solutions for Eq. (59) which corresponds to local minima in the free-energy. One is associated with $S = 0$ and corresponds to an isotropic liquid. The other one with $S > 0$ corresponds to a nematic phase. To decide which solution is realized physically, one must compare the values of free-energies associated with both minima.

The nematic–isotropic transition at constant pressure is located by equating the pressure and chemical potentials of the two phases,

$$p_{nem}(\eta_{nc}, T_c, S_c) = p_{iso}(\eta_{ic}, T_c), \tag{60}$$

$$\mu_{nem}(\eta_{nc}, T_c, S_c) = \mu_{isco}(\eta_{ic}, T_c), \tag{61}$$

with S_c determined by Eq. (59). If the pressure is kept fixed, we have, in fact, four equations in the four unknowns η_{nc}, η_{ic}, T_c and S_c.

7. RESULTS AND DISCUSSIONS

Figure 3 shows the variation of packing fraction, order parameter, and the relative density changes at the nematic–isotropic transition as a

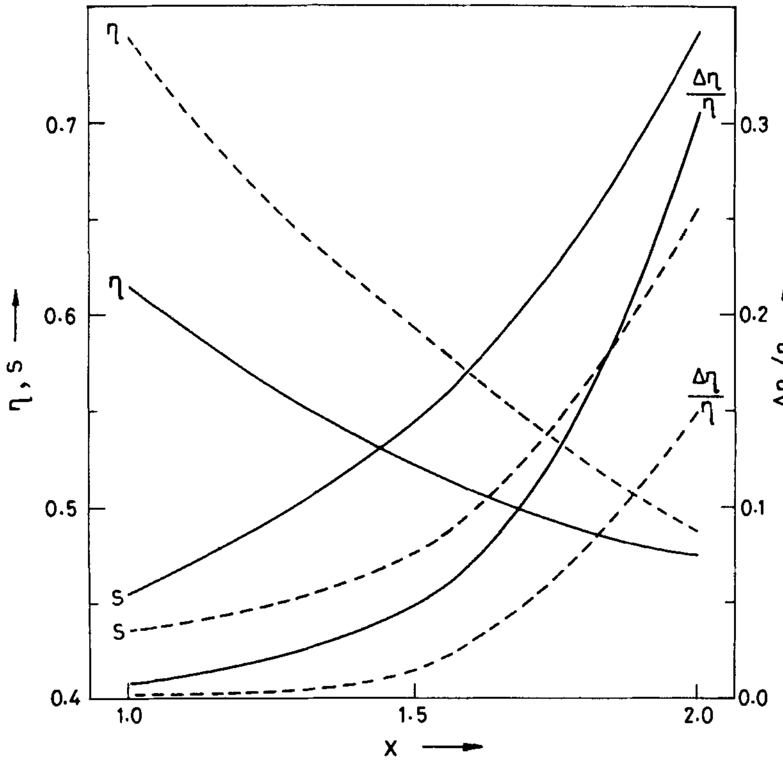

FIGURE 3 The variation of packing fraction η, order parameter S_c and the relative density change $\Delta\eta/\eta$ at the nematic–isotropic transition as a function of x for a given interaction strength $C_i^*/k = 3647.56(K)$, $C_i^*/C_a^* = 8$ (solid line curves), $C_i^*/C_a^* = 50$ (dashed line curves) and the molecular volume $v_0 = 230\ A^3$.

function of x. For this calculations we have used the following values for the interaction parameters and the molecular volume

$$C_i^*/k = 3647.56\ (K),$$

$$C_a^*/C_i^* = 1/8 \text{ and } 1/50, \tag{62}$$

and

$$v_0 = 230(A^{03}).$$

The values of the force parameters and v_0 taken here approximately correspond to those used in the calculation of the nematic–isotropic transition of para-azoxyanisole (PAA) by several workers.[5,10,21] The value of v_0 for PAA was estimated by Viellard-Baron[22] using van der Waals radii and the bond-length from cystallographic data. The value of C_i is estimated from the latent heat of vaporization.[23]

The variation of the transition temperature T_c with the interaction strength C_i^*/k is plotted in Figure 4 for three values of x. In Figure 5 we plot the variation of T_c with the ratio C_a^*/C_i^*. As physically expected our calculation shows (see Figures 4 and 5) that with increasing x the phase transition is shifted to higher temperature, lower density with increasing density change and jump of the order parameter.

Figure 6 shows the packing fraction and the relative change in the density at the transition as a function of C_i^*/C_a^*. In Figure 7 we plot the variation in S as a function of C_i^*/C_a^*. All the values plotted in these figures correspond to the transition temperature $T_c \simeq 409°\text{K}$. We find that the change in the density at the transition decreases as the ratio C_i^*/C_a^* increases for a given value of C_i^*. Though the packing fraction η also increases with C_i^*/C_a^*, the increase is very slow. For $C_i^*/C_a^* \geqslant 20$, we find that the calculated phase transition quantities are not very sensitive to the values of C_i^*/C_a^*. This is in accordance with the observation of Baron and Gelbert.[10] In Table IV we list a number of properties at the nematic–isotropic transition. For a given x and C_a^*/C_i^*, parameter C_i^*/k was chosen so as to reproduce quantitatively the transition temperature T_c which we have taken equal to 409°K. This corresponds to the nematic–isotropic transition temperature for PAA. Though, because of the potential model chosen to represent the pair interaction we do not expect quantitative agreement with any real system, we list in Table IV the values of some of the thermodynamic properties of PAA and PAP at the transition for comparison. In this table the parameter Γ is a measure for the relative sensitivity of the order parameter to volume change (at constant temperature) and

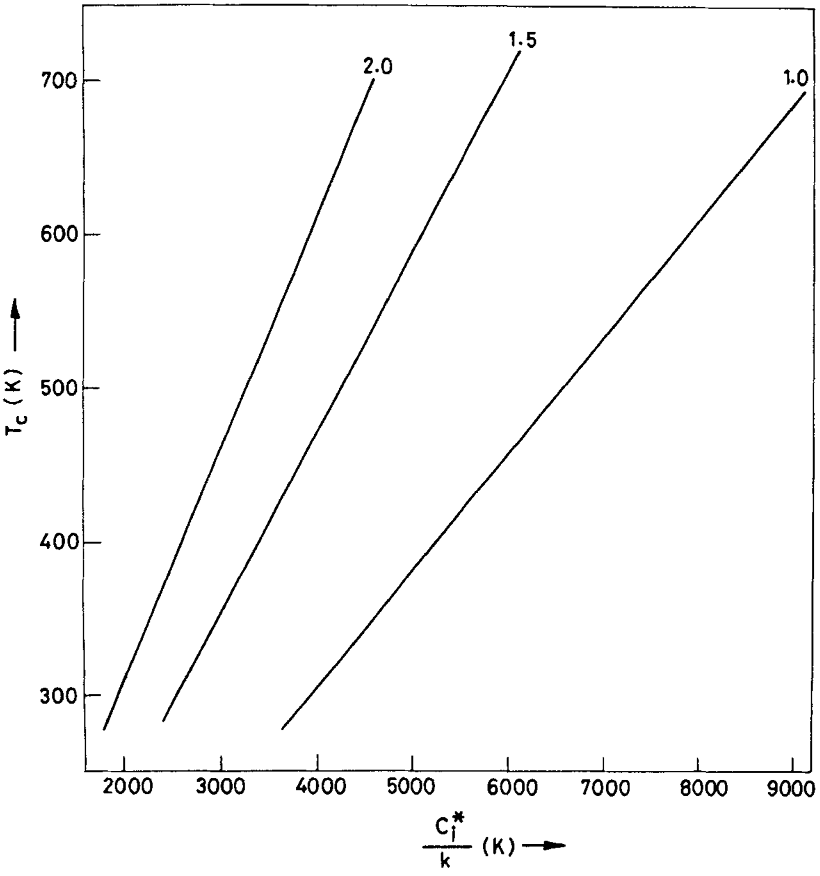

FIGURE 4 The variation of nematic–isotropic transition temperature T_c as a function of C_i^*/k for a fixed value of $C_i^*/C_a^* = 8$. The number on the curves indicates the values of x.

temperature change (at constant volume). It is defined as

$$\Gamma = \frac{V}{T}\frac{(\partial S/\partial V)_T}{(\partial S/\partial T)_V} = -\left(\frac{\partial \ln T}{\partial \ln V}\right)_S = \left(\frac{\partial \ln T}{\partial \ln \rho}\right)_S. \tag{63}$$

The pressure dependence of the transition temperature (dT_c/dp) is obtained by Clausius-Clapeyron's law. $\Delta\Sigma/Nk$ measures the change in entropies at the transition.

As far as the ln T_c-*vs* ln ρ at constant order parameter is concerned, we obtained a straight line for all the cases considered. The slope which are listed in column IX of Table IV are found far from the experimental value of 4.0 for PAA. It may be noted that while for $x = 1$, Γ is

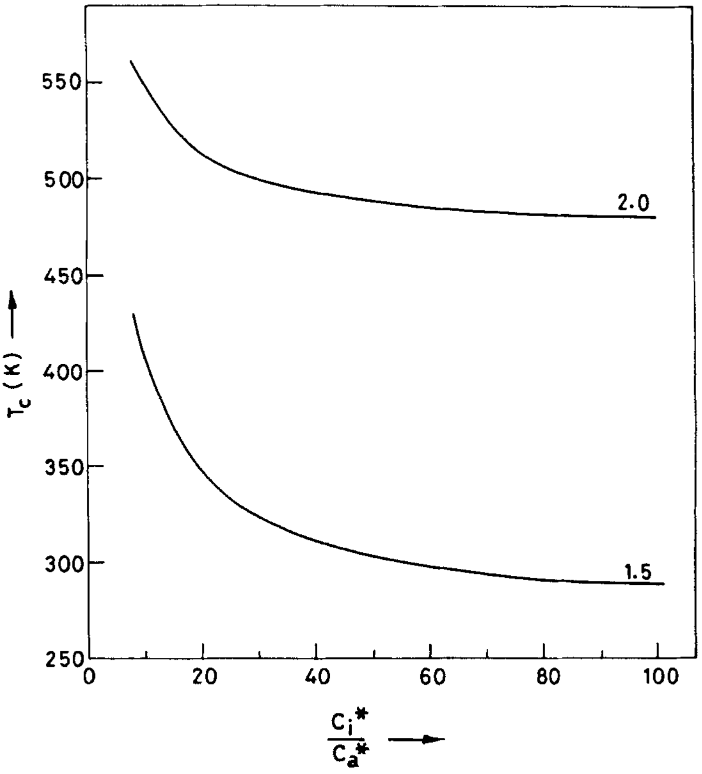

FIGURE 5 The variation of nematic–isotropic transition temperature T_c as a function of C_i^*/C_a^* for a fixed value of $C_i^*/k = 3647.56(K)$. The number on the curves indicates the value of x.

equal to γ_1 defined by Eq. (49); for $x > 1$, $\Gamma > \gamma_1$. The difference $\Gamma - \gamma_1$ is due to coupling between hard-core and attractive interaction. As remarked earlier, for $x = 1$ our theory reduces to the molecular field theory and, therefore, as pointed out by Luckhurst $\Gamma = \gamma_1$.

Figures 8 and 9, respectively, give the temperature dependence of the order parameter S at constant pressure and at constant density. In Figure 8, the experimental values for PAA and PAP are also given. The theoretical curves are given for 1.0 and 1.5. While the theoretical curve for $x = 1$ is close to the experimental values[24-26] of PAA, $x = 1.5$ curve is close to PAP.

As observed experimentally,[27] the calculated nematic–isotropic transition at constant density is shifted to higher temperature as compared to the transition at atmospheric pressure. The experimental values for temperature and pressure for the nematic–isotropic transition for PAA

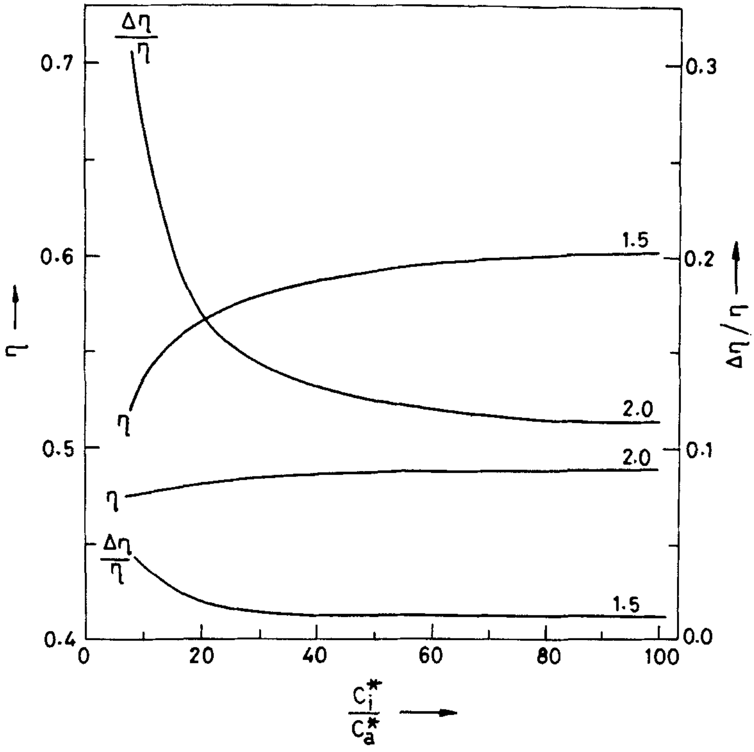

FIGURE 6 The variation of packing fraction η and the relative change in density $\Delta\eta/\eta$ at the transition as a function of C_i^*/C_a^*. C_i^*/k are chosen so as to reproduce the nematic-isotropic transition temperature $T_c \simeq 409(K)$. The number on the curves indicates the values of x.

are 437.5°K and 640 bar whereas our calculation gives, respectively, 425°K and 706.4 bar for $x = 1$ and 447.5°K and 645.7 bar for $x = 1.5$.

As is clear from the table and figures given above we do not find quantitative agreement with experiment for any value of x. It is, however, surprising that relatively better agreement is found for $x = 1$. It is surprising because for PAA, x is expected to be of the order of 3. Attempts have been made to explain this on the basis of microclusters.[21,28] The shape of these microclusters, which consists of a molecule with a few nearest neighbors whose orientations are highly correlated, will resemble a sphere more closely than the shape of a single molecule does. However, such an explanation cannot be taken more seriously than a handwaving argument at present unless, of course, such microclusters arise automatically in a theory.

In most of the calculations[5,10,21,29] reported in past the effective one-

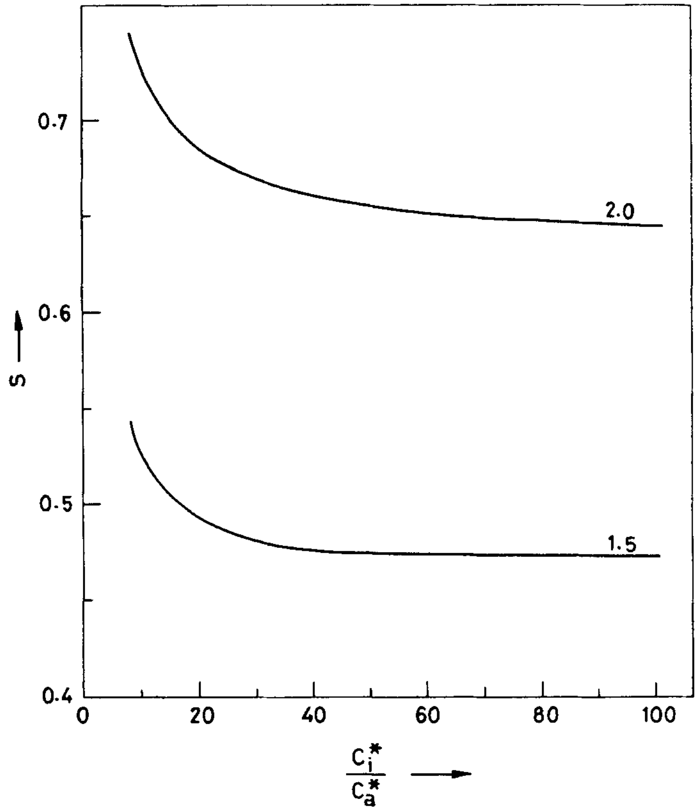

FIGURE 7 The variation of order parameters S at the transition as a function of C_i^*/C_a^*. C_i^*/k are chosen so as to reproduce the nematic–isotropic transition temperature $T_c \simeq 409(K)$. The number on the curves indicates the values of x.

body orientational potential is taken to be of the form,

$$\psi(\cos\theta_1) = -\phi_0^M\rho - \phi_2^M\rho S P_2(\cos\theta_1), \tag{64}$$

where ϕ_0^M and ϕ_2^M are density independent constants. In order to compare and contrast the results of earlier workers with ours, we use this model to calculate the nematic–isotropic transition properties for PAA. The properties of the reference system is evaluated using the formalism of Section 4. The criterion adopted in this calculation for selecting the values of ϕ_0^M and ϕ_2^M was to adjust T_c and the packing fraction η of the nematic phase at T_c to 409°K and 0.62 which are the experimental values for PAA. The results are summarized in Table V.

TABLE IV

The nematic–isotropic transition parameters in the present model system and in p-azoxyanixole (PAA) and p-azoxyphenetole (PAP); S_c is the order parameter; $\bar{\eta} = \frac{1}{2}(\eta + \eta_i)$, η and η_i are nematic and isotropic packing fractions; $\Delta\Sigma/Nk$ the transition entropy, $\Gamma(T_c)$ is defined in Eq. (63). The model parameters are chosen so as to reproduce the transition temperature $T_c \simeq 409°K$.

x	C_i^*/k	C_i^*/C_a^*	$\bar{\eta}$	$\Delta\eta/\eta$	S_c	$\Delta\Sigma/Nk$	(dT_c/dp) $p = 1$ bar	$\Gamma(T_c)$
1.0	5361.91	8	0.612	0.0077	0.454	0.701	30.16 (K/k bar)	1.63
	7321.74	12	0.663	0.0035	0.441	0.605	14.44	1.63
1.5	3472.47	8	0.510	0.0457	0.544	1.266	121.16	1.94
	4311.41	20	0.561	0.0193	0.491	0.870	66.68	2.17
	4902.32	50	0.588	0.0130	0.475	0.756	49.04	2.35
	5164.94	100	0.599	0.0113	0.470	0.722	43.72	2.42
	5471.34	∞	0.610	0.0097	0.466	0.690	38.68	2.59
2.0	2662.72	8	0.403	0.306	0.747	3.946	391.3	2.26
	2912.24	20	0.441	0.163	0.684	2.599	259.3	2.41
	3048.32	50	0.457	0.125	0.655	2.194	223.4	2.52
	3100.43	100	0.462	0.114	0.645	2.069	212.19	2.56
	3155.14	∞	0.468	0.104	0.635	1.948	201.21	2.60
PAA			0.6189	0.0035	0.40 0.36	0.218	43	~4.0
PAP			0.5179	0.0060	0.473 0.520	0.409		

In this table we also list the results reported by Ypma and Vertogen,[21] and Savithramma and Madhusudana.[29]

It may be mentioned that while Ypma and Vertogen[29] have used deformed hard-sphere model and the Bellemann[30] type expansion to calculate the properties of the reference system, Savithramma and Madhusudana[29] have used SPT.[5] These authors have also extended a method given by Andrews[31] for hard spheres to calculate the properties of hard spherocylinders. The value of x given in Table V for the Ypma and Vertogen[21] calculation was obtained from the relation (2·40) of their paper. All these methods differ only in the evaluation of the properties of the reference system and are identical as far as the treatment of the attractive interactions are concerned.

It may be seen from the table that the values reported by Savithramma and Madhusudana[29] and ours are almost identical and are in good agreement with experiment. Such an agreement has been taken to be satisfactory in the literature.[21,29] It is argued that the difference in the theoretical and experimental values of S_c, $\Delta\eta/\eta$ and $\Delta\Sigma/Nk$ are mainly due to the neglect of short-range correlations.

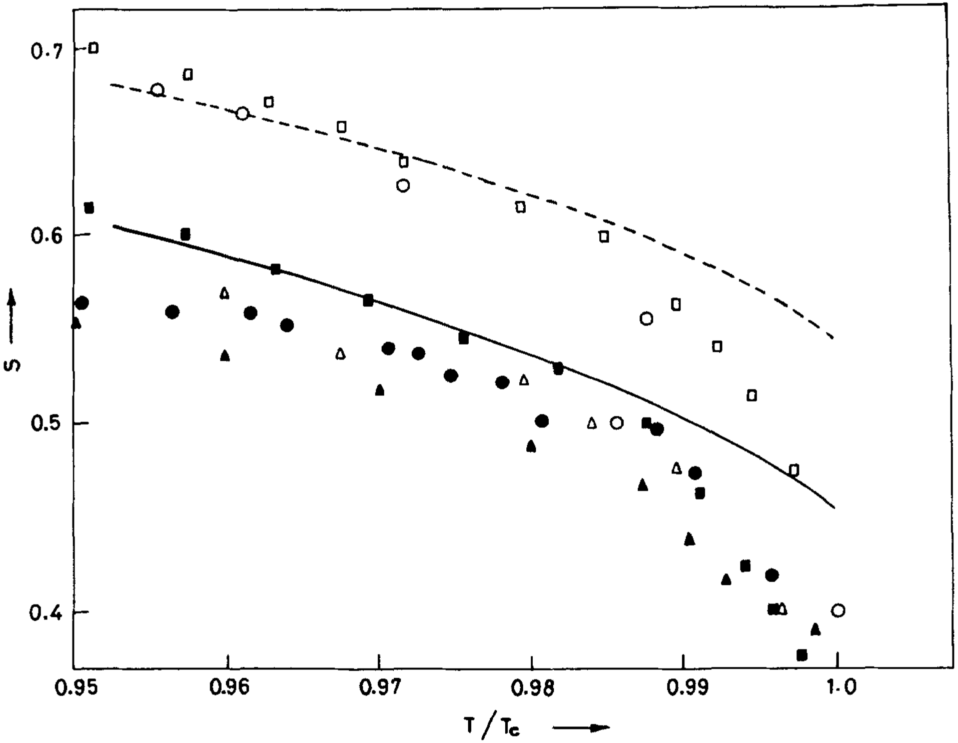

FIGURE 8 The temperature variation of the long-range orientational order parameter S at constant pressure in PAA and PAP. The theoretical curves correspond to: $x = 1.0$, $C_i^*/k = 5361.91(K)$, $C_i^*/C_a^* = 8$, ——— and $x = 1.5$, $C_i^*/k = 3472.47(K)$, $C_i^*/C_a^* = 8$, - - - - - -. The experimental points are the observed values of Rowell *et al.*[22]—Ortho Proton proton splitting (● PAA, ○ PAP); Pines and Change[23]—para carbon—13 chemical shift (■ PAA, □ PAP) and de Jeu and Claassen[24]—magnetic susceptibility (▲ PAA, △ PAP).

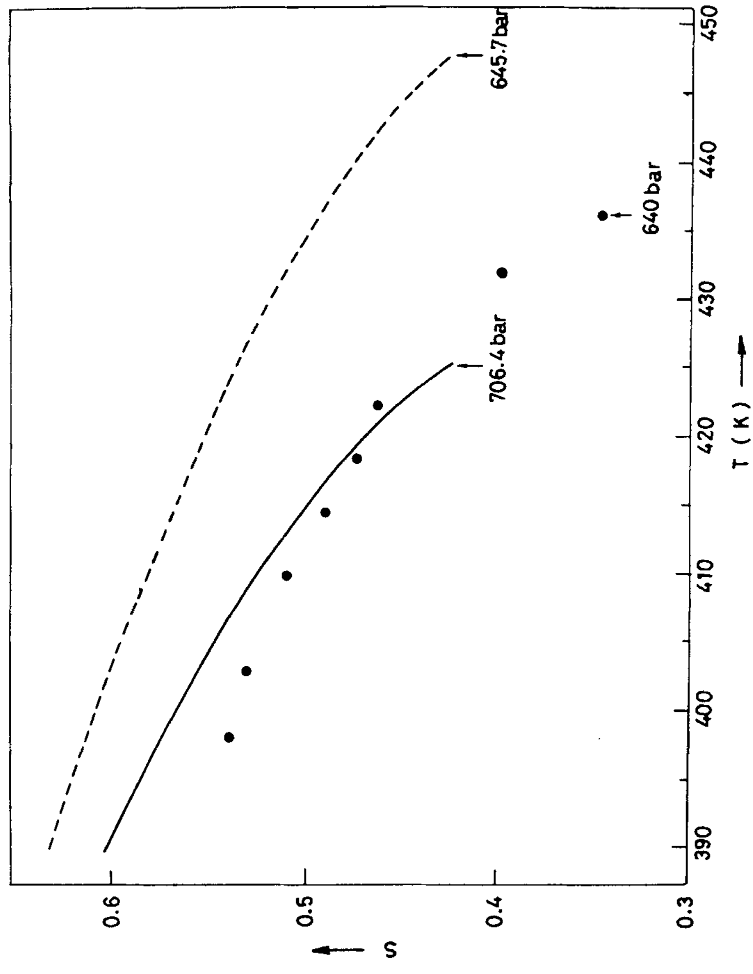

FIGURE 9 The temperature variation of the long-range orientational order parameter S at constant density in PAA. The line symbols for the theoretical curves are the same as that of Figure 8. The experimental points are those of McColl and Shih,[25] from NMR measurements.

TABLE V

Comparison of the nematic–isotropic transition parameters in *p*-azoxyanisole (PAA) and in the model systems.

Quantity	Present work	Ypma and Vertogen[21]	SPT[29]	Modified andrews methods[30]	Experimental PAA
χ	1.80	~1.46	1.75	2.0	~2.7
ϕ_0^M/v_0k	46058(*K*)	39000	54171.07	49590.374	
ϕ_0^M/ϕ_2^M	28.75	21.08	30.70	30.79	
T_c	409°K	409	409	409	409
η	0.62	0.596	0.62	0.62	0.62
η_i	0.6158	0.5899	0.6165	0.6167	0.6178
$\Delta\eta/\eta$	0.0067	0.0102	0.0057	0.0062	0.0035
S_c	0.4571	0.473	0.4548	0.4549	~0.36
$\Delta\Sigma/Nk$	0.4883	0.590	0.5084	0.4846	0.218
(dT_c/dp)	37.24	48.6	—	—	43
$p = 1$ bar	K/k bar				
$\Gamma(T_c)$	4.0	3.96	3.938	3.939	~4.0

From the discussions presented in Sections 2 and 5, it is, however, obvious that Eq. (64) has no theoretical basis. It may be recalled that this relation has emerged from the Maier–Saupe development[32] of a molecular model based upon anisotropic dispersion forces and Cotter's[6] assertion that $\psi(\cos\theta)$ must be proportional to ρ in order to satisfy the statistical mechanical self-consistency. Both these basis have been found incorrect.[4] In Section 5 we have shown that the orientational dependence of $\psi(\cos\theta)$ originates mainly from the coupling between isotropic attractions and anisotropic hard-core repulsions. Using a different analysis, Gelbert and Gelbert[33] have also reached to the same conclusion.

Before concluding we wish to emphasize that the theory developed in this paper should be extended to include,

(i) softness in the repulsive core in the pair potential,

(ii) the dependence of the pair potential on $\hat{r}\cdot\hat{\Omega}$[3]

(iii) the higher-order terms in $\psi(\cos\theta)$, and

(iv) dependence of the pair correlation function on $f(\Omega)$,

before it is applied to explain and predict the observed behavior of the nematic–isotropic transition for real systems. Further, the fluctuations which are expected to play important role near the transition temperature, have also to be included. We hope to discuss some of these problems in our next communication.

References

1. G. W. Gray, *In the molecular physics of liquid crystals,* (ed. by G. R. Luckhurst and G. W. Gray, Acad. Press, London) Chapt. 1 (1979).
2. C. W. Oseen, *Trans. Faraday Soc.,* **29,** 883 (1933).
3. V. T. Rajan and C. W. Woo, *Phys. Rev.,* **A17,** 382 (1978); L. Senbetu and C. W. Wood, *Phys. Rev.,* **A17,** 1529 (1978) and references contained in it.
4. Y. Singh, to be published.
5. M. A. Cotter, *J. Chem. Phys.,* **66,** 1098 (1977).
6. M. A. Cotter, *J. Chem. Phys.,* **67,** 4268 (1977).
7. Y. Singh, *Molec. Phys.,* **29,** 155 (1975).
8. K. P. Shukla, S. Singh and Y. Singh, *J. Chem. Phys.,* **70,** 3086 (1979).
9. G. R. Luckhurst, *In the molecular physics of liquid crystals,* (ed. by G. R. Luckhurst and G. W. Gray, Acad. Press, London) Chapt. 4 (1979).
10. W. M. Gelbert and B. A. Baron, *J. Chem. Phys.,* **66,** 207 (1977); 5795 (1977).
11. L. Verlet and J. J. Weis, *Phys. Rev.,* **A5,** 939 (1972); J. D. Weeks, D. Chandler and H. C. Anderson, *J. Chem. Phys.,* **54,** 5237 (1971).
12. For an excellent review on the perturbation method applicable to isotropic liquid see, J. A. Barker and D. Henderson, *Rev. Mod. Phys.,* **48,** 587 (1976) and J. P. Hansen and I. R. McDonald, *Theory of Simple Liquids* (Acad. Press, New York) Chapt. 6 (1976).
13. L. Onsager, *Ann. N.Y. Acad. Sci.,* **51,** 627 (1949); A. Ishihara, *J. Chem. Phys.,* **19,** 1142 (1951); R. Zwanzig, *J. Chem. Phys.,* **39,** 1714 (1963); L. Runnels and C. Calvin, *J. Chem. Phys.,* **53,** 4219 (1970).
14. P. J. Flory, *Proc. R. Soc. London,* **A234,** 73 (1976); M. A. Cotter and D. E. Martire, *Mol. Cryst. Liq. Cryst.,* **7,** 295 (1969); R. Alben, *Mol. Cryst. Liq. Cryst.,* **13,** 193 (1971).
15. D. Chandler and H. C. Anderson, *J. Chem. Phys.,* **57,** 1930 (1972); D. Chandler, *J. Chem. Phys.,* **59,** 2742 (1973); E. Johnson, *J. Chem. Phys.,* **67,** 3194 (1977) and other references contained in it.
16. M. A. Cotter and D. C. Wacker, *Phys. Rev.,* **A. 18,** 2669, 2676 (1978).
17. J. D. Parson, *Phys. Rev.,* **A19,** 1225 (1979).
18. P. A. Mason and M. Rigby, *Molec. Phys.,* **35,** 1337 (1978).
19. B. J. Berne and P. Puchukas, *J. Chem. Phys.,* **56,** 4213 (1972).
20. B. Larsen, J. C. Rasaiah and G. Stell, *Molec. Phys.,* **33,** 987 (1977).
21. J. G. J. Ypma and G. Vertogen, *Phys. Rev.,* **A17,** 1490 (1978).
22. J. Viallard-Baron, *Molec. Phys.,* **28,** 809 (1974).
23. J. Solsky and E. Grushka, *J. Phys. Chem.,* **78,** 275 (1974).
24. J. C. Rowell, W. D. Philips, L. R. Melby and M. Panar, *J. Chem. Phys.,* **43,** 3442 (1965).
25. A. Pines and J. J. Chang, *J. Am. Chem. Soc.,* **96,** 5590 (1974).
26. W. H. de Jeu and W. A. P. Claassen, *J. Chem. Phys.,* **68,** 102 (1978).
27. J. R. McColl and C. S. Shih, *Phys. Rev. Lett.,* **29,** 85 (1972).
28. P. Sheng, *J. Chem. Phys.,* **59,** 1942 (1973); G. R. Luckhurst and C. Zannoni, *Nature Lond.,* **267,** 412 (1977).
29. K. L. Savithramma and N. V. Madhusudana, *Mol. Cryst. Liq. Cryst.,* **62,** 63 (1980).
30. A. Bellemans, *Phys. Rev. Lett.,* **21,** 527 (1968).
31. F. C. Andrews, *J. Chem. Phys.,* **62,** 272 (1975).
32. W. M. Maier and A. Saupe, *Z. Naturforsch,* **A14,** 882 (1959); **A15,** 287 (1960).
33. W. M. Gelbert and A. Gelbert, *Molec. Phys.,* **33,** 1387 (1977).